EXPERIMENTS USING HIGH-T_C VERSUS LOW-T_C JOSEPHSON CONTACTS

Ariando,[1] H. J. H. Smilde,[1] C. J. M. Verwijs,[1] G. Rijnders,[1] D. H. A. Blank,[1] H. Rogalla,[1] J. R. Kirtley,[2] C. C. Tsuei,[2] and H. Hilgenkamp[1]
(h.hilgenkamp@utwente.nl)
[1]*Faculty of Science and Technology and MESA+ Institute for Nanotechnology, University of Twente, P.O. Box 217, 7500 AE Enschede, The Netherlands*
[2]*IBM T. J. Watson Research Center, Yorktown Heights, New York 10598, USA*

Abstract. Remarkably rich physics is involved in the behavior of hybrid Josephson junctions, connecting high-T_c and low-T_c superconductors. This relates in particular to the different order parameter symmetries underlying the formation of the superconducting states in these materials. Experiments on high-T_c/low-T_c contacts have also played a crucial role in settling the decade-long *d*-wave versus *s*-wave debate in cuprate superconductors. Recently, such hybrid junctions have enabled more detailed pairing symmetry tests. Furthermore, with these junctions, complex arrays of π-rings have been realized, enabling studies on spontaneously generated fractional flux quanta and their mutual interactions. Steps toward novel superconducting electronic devices are taken, utilizing the phase-shifts inherent to the *d*-wave superconducting order parameter. This paper is intended to reflect the current status of experiments using high-T_c and low-T_c Josephson contacts.

Key words: Josephson junctions, hybrid junctions, pairing symmetry, high-temperature superconductors, half-flux quanta

1. Introduction

The introduction of additional phase shifting elements in superconducting loops leads to remarkable effects (van Harlingen, 1995; Tsuei and Kirtley, 2000a). This can be achieved e.g. by using superconductors with unconventional pairing symmetry (Geshkenbein and Larkin, 1986; Geshkenbein et al., 1987; Sigrist and Rice, 1992; Tsuei and Kirtley, 2000a), by incorporating π-Josephson junctions (Bulaevskii et al., 1977), or by employing trapped flux quanta (Majer et al., 2002) or current injection (Goldobin et al., 2004). In phase-sensitive tests of the pairing symmetry, superconductors with unconventional pairing symmetry were used to create a π phase-shift in the ring (π-ring), leading to a complementary magnetic field dependence of the critical current of the ring (Wollman et al., 1993; Wollman et al., 1995) and to the half-flux quantum effect (Tsuei et al., 1994).

These interesting observations are due to the physics associated with *d*-wave symmetry taking place at the interface of the high-T_c cuprate superconductors, as

reviewed for example in (van Harlingen, 1995; Tsuei and Kirtley, 2000a; Kashiwaya and Tanaka, 2000; Hilgenkamp and Mannhart, 2002; Tafuri and Kirtley, 2005). Other interesting phenomena primarily associated with *d*-wave symmetry include e.g. Andreev bound states (Hu, 1994; Kashiwaya and Tanaka, 2000; Chesca et al., 2005; Chesca et al., 2006), the presence of the second harmonic in the critical current versus phase relation (Golubov et al., 2004), or vortex splintering (Mints et al., 2002).

In the phase-sensitive experiments, superconducting loops were fabricated using a high-T_c cuprate connected to a low-T_c superconductor (Wollman et al., 1993; Wollman et al., 1995), or using tricrystal or tetracrystal grain boundary junctions (Tsuei et al., 1994; Tsuei and Kirtley, 2000a). In this article we will concentrate only on the first route, using a high-T_c material connected to a low-T_c superconductor.

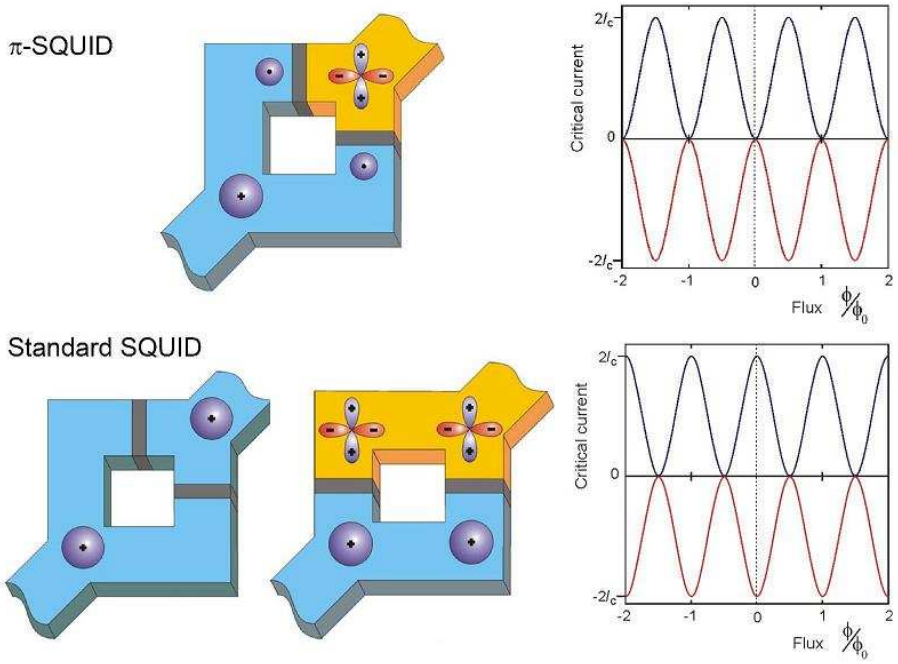

Figure 1. (Color) A schematic representation of a π-ring (top) and a 0-ring (bottom), and the expected magnetic field dependencies of their critical currents as shown at the right-hand side.

A schematic of a π-ring (π-SQUID) and 0-ring (standard SQUID) employing high-T_c and low-T_c Josephson contacts is depicted in Fig. 1. In the limit of a low inductance $L \ll \Phi_0/I_c$, with $\Phi_0 = h/2e = 2.07 \times 10^{-15}$ Wb the flux quantum and I_c the critical current of the junctions in the ring, the π-SQUIDs have $I_c(B)$ characteristics complementary to those of standard SQUIDs. For $L \gg \Phi_0/I_c$,

the energetic ground state involves a spontaneously generated flux of $\frac{1}{2}\Phi_0$ in the SQUID loop. To compensate for the built-in π-phase shift a spontaneous circulating current flows in the ring, in either the clock- or counter-clockwise direction. The magnetic flux associated with this persistent circulating current is a fraction of a flux quantum, growing asymptotically to a half-flux quantum in the large inductance limit (Kirtley et al., 1997). In the limiting case when the inner diameter of the π-ring in Fig. 3 is reduced to zero, the structure represents the corner junction (Wollman et al., 1995). A corner junction behaves similarly to a π-ring. In this structure, the *d*-wave order parameter of the high-T_c cuprate induces a difference of π in the Josephson phase shift $\Delta\phi$ between the two junctions (facets). For facet lengths a in the small limit, that is, $a \ll \lambda_J$, the corner junction has $I_c(B)$ characteristics with zero critical current in the absence of magnetic fields, in stark contrast to the Fraunhofer pattern for a uniform junction. For facet lengths a in the wide limit, that is, $a \gg \lambda_J$, the lowest-energy ground state of the system is expected to be characterized by the spontaneous generation of a half-integer flux quantum at the corner. This half-fluxon provides a further π-phase change between neighbouring facets, either adding or subtracting to the *d*-wave induced π-phase shift, depending on the half-flux-quantum polarity. In both cases, this leads to a lowering of the Josephson coupling energy across the barrier, as this energy is proportional to $(1 - \cos\Delta\phi)$.

2. Preparation of high-T_c and low-T_c ramp-type Josephson contacts

Various early attempts have been made to prepare Josephson contacts between high-T_c and low-T_c superconductors, such as $YBa_2Cu_3O_7$ (YBCO) and Nb (Akoh et al., 1988; Akoh et al., 1989; Akoh et al., 1990; Fujimaki et al., 1990; Fujimaki et al., 1991; Hunt et al., 1990; Hunt et al., 1991; Foote et al., 1991; Terai et al., 1993; Wollman et al., 1993; Brawner and Ott, 1994a; Brawner and Ott, 1994b; Mathai et al., 1995; Gim et al., 1996; Wollman et al., 1995; Terai et al., 1995; Brawner and Ott, 1996; Usagawa et al., 1998). Oxygen migration due to the chemical reactivity of Nb with oxygen, combined with the sensitivity of YBCO to oxygen loss, presents a difficulty for the preparation of a good electrical connection between both superconductors. Another crucial step, especially using the ramp type configuration, is the structuring of the superconducting base electrode. Unfortunately, this procedure can severely degrade the quality of the base electrode near the interface. Transmission electron microscopy (TEM) studies of YBCO/Au ramp-type interfaces (Wen et al., 1999) clearly show an amorphous layer with a thickness up to 2 nm at the ramp edge between the high-T_c base electrode and the Au layer deposited at the freshly milled ramp edge.

Using the ramp-type interface configuration (Gao et al., 1990; Gao et al., 1991; Verhoeven et al., 1996), we have been able to establish a fabrication procedure (Smilde et al., 2002b) for all-thin-film Josephson junctions, in which con-

trollably a high-T_c cuprate superconductor (such as YBCO or $Nd_{2-x}Ce_xCuO_4$ (NCCO)) is connected with a low-T_c material (Nb) along freely chosen directions of the high-T_c cuprates. A thin interlayer is incorporated in the junctions to obtain an increased transparency. The interlayer restores the surface damaged by ion milling and has the advantage of an in-situ barrier deposition between the two superconductors, leading to clean and well-defined interfaces. To avoid oxygen migration at the interface, a thin but chemically closed barrier separating the materials is used, for which Au is found to be the most suitable material (Smilde et al., 2001a; Smilde et al., 2001b).

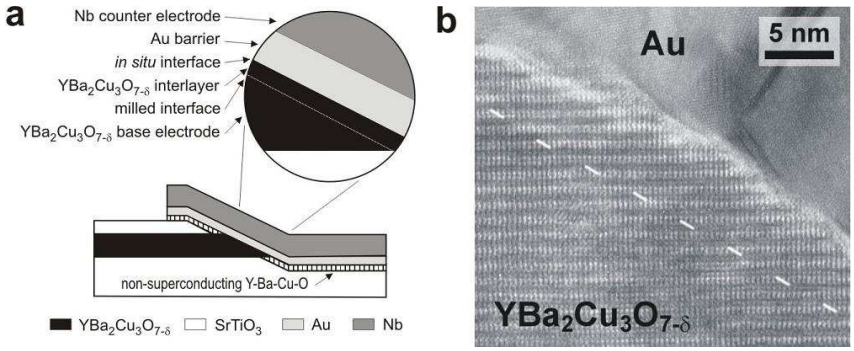

Figure 2. (a) Schematic cross section of the $YBa_2Cu_3O_{7-\delta}$/Au/Nb ramp-type junction including the interlayer. (b) Bright-field transmission electron microscopy image of the $YBa_2Cu_3O_{7-\delta}$/Au interface at the ramp-edge area, including an interlayer of 6 nm deposited $YBa_2Cu_3O_{7-\delta}$. Crystalline $YBa_2Cu_3O_{7-\delta}$ material is observed up to the Au interface, while no clear interface is observed between the base electrode and the interlayer (dashed line) [from (Smilde et al., 2002b)].

For the preparation, first a [001]-oriented high-T_c cuprate and a $SrTiO_3$ insulator layer are epitaxially grown by pulsed laser deposition (PLD) on [001]-oriented $SrTiO_3$ single crystal substrates. In these films, beveled edges (ramps) are etched by Ar-ion milling under an angle of 45° using a photoresist stencil, yielding ramps with an angle of $\sim$ 20° with the substrate plane (Blank and Rogalla, 1997). In order to facilitate a good alignment of the junction with the ⟨100⟩-axes of the high-T_c film, edge-aligned substrates are used, with an alignment accuracy better than 1°. After stripping of the photoresist, a low-voltage ion mill step is applied to clean the surface, in-situ followed by an annealing step and the deposition of a thin interlayer of 5 – 7 nm YBCO at a condition similar to the deposition of the YBCO base-electrode. The annealing procedure is introduced to recrystallize residual amorphous material present at the ramp edge. This is followed by an in-situ deposition of Au-barrier at room temperature. After deposition of the Au-barrier layer with a thickness ranging from 6 to 120 nm, a photoresist lift-off stencil is applied to define the junction area. Before Nb deposition, maximally 2 nm of the Au layer is removed by rf-sputter etching, followed in situ by dc-

sputter deposition of 150 nm Nb. After lift-off, the redundant uncovered Au is removed using ion milling.

A schematic of the junction obtained in this way is presented in Fig. 2a. The interlayer concept employs the difference in homoepitaxial and heteroepitaxial growth of high-T_c material. The thin interlayer is anticipated to be superconducting only if deposited on the YBCO ramp area, whereas on the $SrTiO_3$ substrate and isolation layer it is anticipated not to become superconducting (Smilde et al., 2002b). Figure 2b presents a TEM micrograph of the ramp edge area near the YBCO/Au interface. Because of the application of the thin YBCO interlayer, crystalline high-T_c material extends up to the Au barrier, and an amorphous layer was never observed. The interface between the base electrode and the interlayer could not be distinguished by TEM, indicating nearly perfect homoepitaxial growth.

Following this procedure results in normal state resistance R_nA values of $\sim 10^{-12}$ Ωm^2 at liquid helium temperature. By adapting the Au-barrier thickness d_{Au}, the junction critical current density can be tuned in a wide range from 10^5 A/m^2 for $d_{Au} \sim 120$ nm, up to values approaching 10^9 A/m^2 for $d_{Au} \sim 7$ nm. In the following, we will review recent experiments based on high-T_c versus low-T_c contacts prepared using the procedure that has been described in this section.

3. Pairing symmetry test experiments

Understanding the nature of the ground state and its low-lying excitations in the copper oxide superconductors is a prerequisite for determining the origin of high temperature superconductivity. A superconducting order parameter (that is, the energy gap) with a predominantly $d_{x^2-y^2}$ symmetry is well-established (van Harlingen, 1995; Tsuei and Kirtley, 2000a). There are, however, several important issues that remain highly controversial. For example (in hole-doped compound such as YBCO) various deviations from a pure d-wave pair state, such as the possibility of Cooper pairing with broken time-reversal symmetry (BTRS) or an admixed $d_{x^2-y^2} + s$ pair state, have been theoretically predicted (Laughlin, 1988; Varma, 1999; Sigrist, 1998; Lofwander et al., 2001) and actively sought in numerous experimental studies (Spielman et al., 1992; Lawrence et al., 1992; Kaminski et al., 2002; Varma, 2002; Fauque et al., 2005; Covington et al., 1997; Dagan and Deutscher, 2001; Sharoni et al., 2002; Mathai et al., 1995; Schulz et al., 2000). Furthermore, a transition of the pairing symmetry from d-wave behavior to s-wave-like behavior was also suggested as a function of doping (Skinta et al., 2002; Biswas et al., 2002; Qazilbash et al., 2003) and temperature (Balci and Greene, 2004) in various electron doped compounds.

In view of this ongoing discussion, there is a need for further phase-sensitive experiments as a function of doping and temperature, and specifically for studying the possible existence of BTRS states. Many phase-sensitive experiments have been performed to look for evidence of BTRS (van Harlingen, 1995; Tsuei and

Kirtley, 2000a; Mathai et al., 1995; Schulz et al., 2000). From these it has been concluded that, if present, the imaginary component must be quite small for high-T_c cuprates over a broad range of doping (Tsuei et al., 2004). Tsuei and Kirtley succeeded in performing phase-sensitive measurements for various compounds and temperatures based on grain boundary junctions and half-flux quantum effects (Tsuei and Kirtley, 2000a). Geometrical restrictions of the grain boundaries makes such experiments very challenging, especially for investigations as a function of momentum. In this section we describe various phase-sensitive experiments that have been performed based on high-T_c/Nb Josephson contacts.

3.1. LOW-INDUCTANCE-SQUID INTERFEROMETRY

Superconducting quantum interference devices present excellent tools to perform phase-sensitive experiments on the order parameter symmetry in superconductors (Wollman et al., 1993; Brawner and Ott, 1994a; Mathai et al., 1995; van Harlingen, 1995; Schulz et al., 2000). In a dc SQUID in which an isotropic *s*-wave superconductor contacts the superconductor to be studied in two crystal orientations, the critical current versus the applied magnetic flux dependence contains information about the relative phase and magnitude of the order parameter wave function at both contacts. Previous SQUID experiments on the order parameter symmetry of the high-T_c cuprates have been performed using, for example, Pb as a counter electrode. In these experiments, single crystals (Brawner and Ott, 1994a) as well as twinned and untwinned thin films (Wollman et al., 1993; Mathai et al., 1995) of $YBa_2Cu_3O_7$ have been used. These SQUIDs generally had inductances of $LI_c \approx \Phi_0$ or larger.

Low-inductance SQUIDs enable a more precise analysis (Schulz et al., 2000; Smilde et al., 2004a). Low-inductance all-high-T_c π-SQUIDs have been prepared using tetra-crystal substrates, providing clear evidence for predominant $d_{x^2-y^2}$-wave order parameter symmetry (Schulz et al., 2000). These dc π-SQUIDs were based on symmetric 45° [001]-tilt grain-boundary junctions. By definition, grain-boundary junctions are subject to limitations with respect to the orientation of the superconductors on both sides of the junction interface. Additionally, a complicating factor is presented by the fact that both electrodes are characterized by the order parameter symmetry under investigation. Junctions combining a well-characterized isotropic superconductor with the superconductor to be studied provide the ability to probe the order parameter in any desired orientation.

We have fabricated low-inductance SQUIDs based on high-T_c versus low-T_c Josephson contacts. Sketches of the devices are shown in the insets of Fig. 3. If the high-T_c order parameter is probed by an isotropic superconductor along the same main crystal orientation in a dc SQUID (bottom), i.e., both junctions are oriented in parallel, a maximum critical current is then observed in the absence of an applied magnetic field as shown in Fig. 3 (bottom). When the junctions are ori-

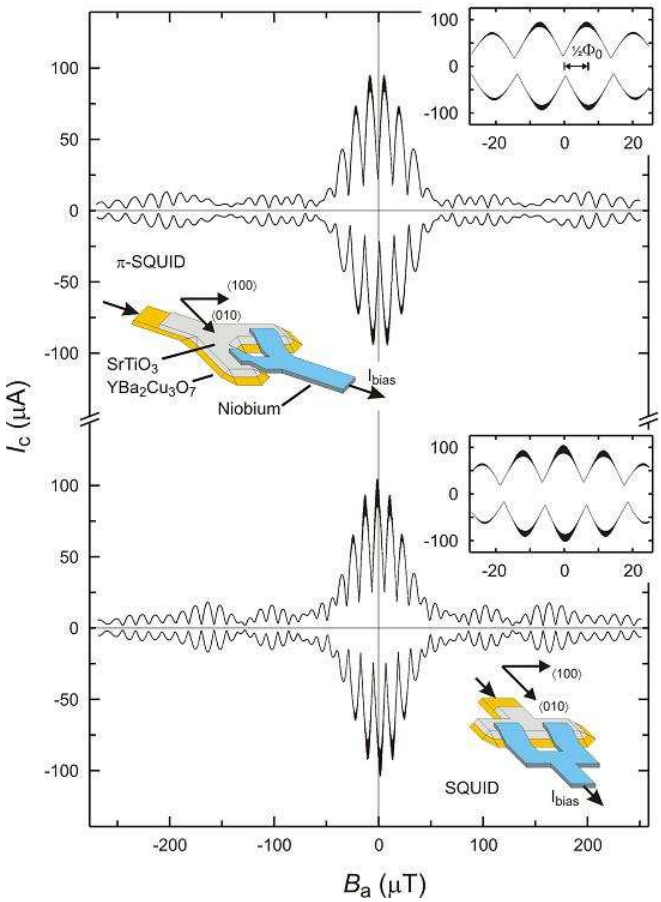

Figure 3. (Color) Critical current as a function of the applied magnetic field at $T = 4.2$ K of a π-SQUID (top) and standard SQUID (bottom). The insets present schematically the corresponding configuration and an enlargement of the $I_c(B)$ dependence near zero field. Both SQUIDs are in the low inductance limit [from (Smilde et al., 2004a)].

ented perpendicular with respect to each other in the [100]-directions, the high-T_c order parameter symmetry induces an additional phase-shift in the SQUID-loop. A time reversal invariant $d_{x^2-y^2}$ order parameter symmetry of the high-T_c cuprate corresponds to a π phase-shift, and maxima in the critical current are observed at a magnetic field equivalent to $\frac{1}{2}\Phi_0$ as depicted in Fig. 3 (top). A time-reversal symmetry breaking (TRSB) order parameter, such as predominant $d_{x^2-y^2}$ pairing with an imaginary *s*-wave admixture, results in a deviation from π, and consequently the maximum critical current occurs at an applied flux differing from $\frac{1}{2}\Phi_0$. Therefore no evidence has been found for imaginary admixtures. Twinning of the film prevents the determination of possible real admixtures.

3.2. JOSEPHSON JUNCTION MODULATION

Multiple π-loops placed controllably at arbitrary positions would enable more detailed and systematic studies of the order parameter symmetry and its effects on Josephson devices (Smilde et al., 2002a; Ariando et al., 2005), as well as the realization of theoretically proposed elements for superconducting (quantum) electronics (Terzioglu and Beasley, 1998; Ioffe et al., 1999; Blatter et al., 2001).

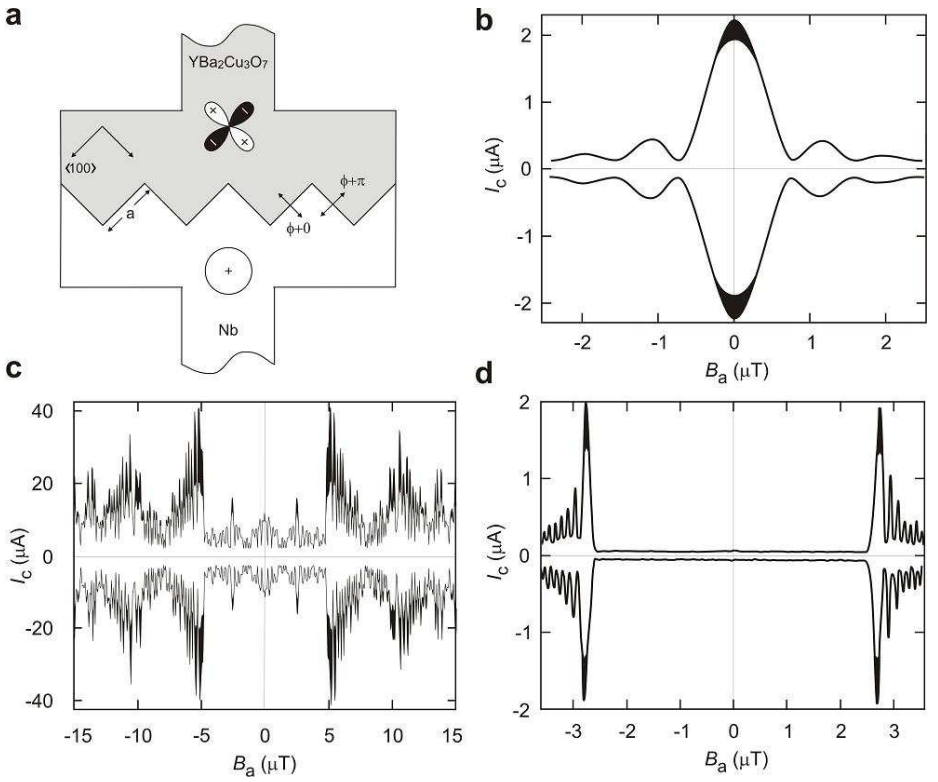

Figure 4. (a) A schematic representation of a zigzag junction. Critical current I_c as a function of applied magnetic field B_a for (b) a straight junction, and (c) a YBCO/Nb and (d) a NCCO/Nb zigzag array comprised of 80 facets of 5 μm width (T = 4.2 K) [from (Smilde et al., 2002a) and (Ariando et al., 2005)].

We have fabricated well-defined zigzag-shaped ramp-type Josephson junctions between various high-T_c superconductors and Nb, and used such structures to test the order parameter symmetry of these high-T_c compounds. The zigzag configuration is depicted in Fig. 4a. In this structure, all interfaces are aligned along one of the ⟨100⟩ directions of the cuprate, and are designed to have identical critical current density (J_c) values. If the high-T_c cuprate were an *s*-wave superconductor, there would be no significant difference between a zigzag and

a straight junction, aligned along one of the facet′s direction. With the high-T_c superconductor having a $d_{x^2-y^2}$-wave symmetry, the facets oriented in one direction experience an additional π-phase difference compared to those oriented in the other direction. For a given number of facets, the characteristics of these zigzag structures then depend on the ratio of the facet length a and the Josephson penetration depth λ_J; see, e.g., (Zenchuk and Goldobin, 2004). In the small facet limit, $a \ll \lambda_J$, the zigzag structure can be envisaged as a one-dimensional array of Josephson contacts with an alternating sign of J_c, leading to anomalous magnetic field dependencies of the critical current. In the large facet limit, the energetic ground state includes the spontaneous formation of half-integer magnetic flux quanta at the corners of the zigzag structures, as seen in (Hilgenkamp et al., 2003). All experiments described in this section are in the small facet limit.

Figure 4c and 4d shows the $I_c(B_a)$ dependence for a YBCO/Nb and a NCCO/Nb zigzag array with 80 facets having a facet length of 5 μm, respectively. The $I_c(B_a)$ dependencies of these zigzag structures clearly exhibit the characteristic features with an absence of a global maximum at $B_a(0)$ and the sharp increase in the critical current at a given applied magnetic field, resembling in their basic features the ones observed for asymmetric 45° [001]-tilt grain boundary junctions. This behavior can only be explained by the facets being alternatingly biased with and without an additional π-phase change (Copetti et al., 1995; Hilgenkamp et al., 1996; Mannhart et al., 1996; Mints and Kogan, 1997). This provides a direct evidence for a π-phase shift in the pair wave function for orthogonal directions in momentum space and thus for a predominant $d_{x^2-y^2}$ order parameter symmetry. If the order parameter were to comprise an imaginary s-wave admixture, the $I_c(B_a)$ dependencies for the zigzag junctions would be expected to display distinct asymmetries, especially for low fields (Smilde et al., 2002a). In addition, the critical current at zero applied field is expected to increase with the fraction of s-wave admixture. From the high degree of symmetry of the measured characteristics of Figs. 4c and 4d and the very low zero field I_c, an upper limit of an imaginary s-wave symmetry admixture to the predominant $d_{x^2-y^2}$ symmetry of 1% for YBCO can be set and no indication for subdominant symmetry components for NCCO can be distinguished. The d-wave result for the electron-doped superconductor corroborates the results obtained using grain boundary junctions (Tsuei and Kirtley, 2000b; Chesca et al., 2003)

To investigate a possible change of the order parameter symmetry with doping (Biswas et al., 2002; Qazilbash et al., 2003), we have fabricated similar zigzag structures using $Nd_{1.835}Ce_{0.165}CuO_4$/Nb junctions. The results also indicated a predominant $d_{x^2-y^2}$-wave symmetry. When cooling the samples to $T = 1.6$ K all the basic features displayed by the structures at $T = 4.2$ K remain unaltered. We thus see no indication for an order parameter symmetry crossover for $Nd_{1.835}Ce_{0.165}CuO_4$ in this temperature range, as was reported for $Pr_{2-x}Ce_xCuO_{4-y}$ (Balci and Greene, 2004). Similar results were obtained for optimally doped sam-

ples upon cooling to $T = 1.6$ K.

3.3. ANGLE-RESOLVED ELECTRON TUNNELING

The upper limit of an imaginary *s*-wave symmetry admixture can be determined using the experiments described above. However, these experiments used geometries in which the junction normals are perpendicular to the *a*- and *b*- axes. They are, therefore, insensitive to an imaginary d_{xy} component which has nodes along the *a*- and *b*-axes. Another possible modification of the pure *d*-wave gap parameter is an admixed $d_{x^2-y^2} + s$ pair state, where *s* is the *s*-wave real component of the gap, as required by group theory for the in-plane CuO lattice symmetry of orthorhombic cuprate superconductors such as YBCO (Tsuei and Kirtley, 2000a). Although a $d + s$ pair state in YBCO is established (Polturak et al., 1993; Basov et al., 1995; Rykov and Tajima, 1998; Lu et al., 2001; Engelhardt et al., 1999), reports of the magnitude of the *s*-wave admixture vary. Twinning of the YBCO thin films used in the experiments discussed above prevents the determination of possible real admixtures. To further examine the *d*-wave order parameter symmetry, it is therefore important to perform pairing symmetry tests as a function of in-plane momentum using untwinned films. We have performed such experiments on untwinned optimally-doped YBCO films based on YBCO/Nb contacts (Smilde et al., 2005; Kirtley et al., 2006).

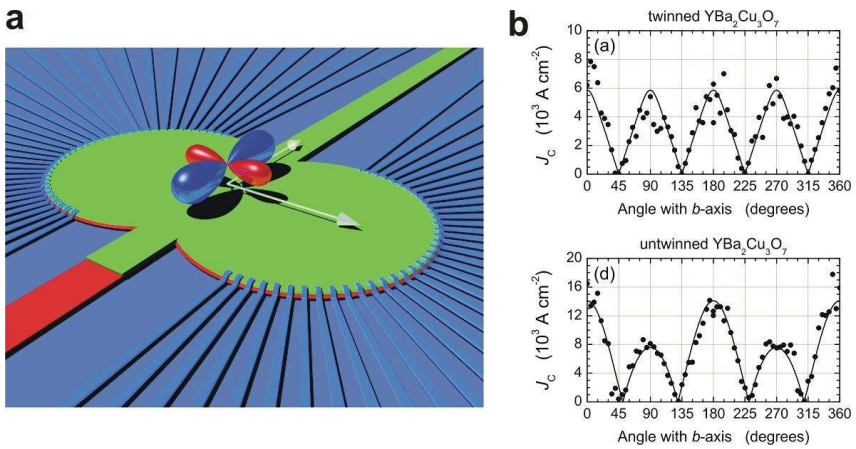

Figure 5. (Color) (a) Angle-resolved electron tunneling with $YBa_2Cu_3O_7$/Au/Nb ramp-type junctions oriented every 5° over 360°. The arrows indicate the main crystal orientations in the *ab* plane of the high-T_c superconducting material. (b) Critical current densities J_c as a function of the junction orientation with respect to the $YBa_2Cu_3O_7$ crystal for (top) twinned and (bottom) untwinned $YBa_2Cu_3O_7$ at $T = 4.2$ K and in zero magnetic field [from (Smilde et al., 2005)].

The experimental layout is summarized in Fig. 5a. Basically, the YBCO base electrode is patterned into a nearly circular polygon, changing the orientation from

side to side by 5°. A Au barrier and Nb counterelectrode contact each side. In this way, the angle with respect to the (010)-orientation is varied as a single parameter. Figure 5b presents the electrical characterization of the twinned base-electrode sample (top), and the untwinned one (bottom). The superconducting properties of the Au/Nb bilayer are independent of the orientation. Therefore, J_c depends on the in-plane orientation θ with respect to the *b*-axis of the YBCO crystal only, and presents four maxima for both samples, approaching zero in between. This is in agreement with predominant $d_{x^2-y^2}$-wave symmetry of the superconducting wave function in one electrode only. In closer detail, the nodes of the untwinned YBCO sample are found at 5° from the diagonal between the *a*- and the *b*-axis. This presents direct evidence for a significant real isotropic *s*-wave admixture. An estimate for the *s*- over $d_{x^2-y^2}$-wave gap ratio is 17% for a node angle $\theta_0 = 50°$, resulting in a gap amplitude 50% higher in the *b* (Cu-O chain) direction than in the *a* direction. For the twinned base electrode, the nodes are found at the diagonal, which is expected if all twin orientations are equally present, and contributions of subdominant components average to zero.

3.4. ANGLE-RESOLVED PHASE-SENSITIVE EXPERIMENTS

Measurements of the critical currents of single YBCO-Nb junctions described above resulted in a gap 50% larger in the *b* than the *a* direction for optimally doped YBCO. To further quantify the deviations from a pure $d_{x^2-y^2}$ symmetry, in particular BTRS states, phase-sensitive experiments as a function of in-plane momentum are needed. Such experiments have been suggested to be sensitive to an imaginary component to the order parameter (Beasley et al., 1994; Ng and Varma, 2004). We have performed phase-sensitive experiments based on two-junction rings connecting YBCO and Nb to be able to accurately determine the in-plane pairing symmetry (Kirtley et al., 2006).

A schematic of the rings for this experiment is shown in Fig. 6a. Each ring has one junction with a fixed angle of $-22.5°$ relative to the majority twin *a*-axis direction in the YBCO, with the second junction angle varying in intervals of 5°. The ring geometries were optimized with several considerations in mind. For this measurement it is desirable to have large rings, because this leads to large I_cL products, so that the spontaneous magnetization is not reduced from the asymptotic $\Phi_0/2$ value. Large rings are also easier to resolve with the SQUID microscope. It is important that the junction interfaces are well-defined, clean and have a sufficiently high critical current density.

Figure 6 shows a SQUID microscope image of one of the rings, cooled and imaged in zero field. The spontaneous flux is clearly visible in the center of the ring; the ring walls are nearly invisible. Figure 6b shows images of the rings in this sample, cooled and imaged in zero field, depicted as a polar plot. This underlines the nearly four-fold symmetry of the data, with the transitions between 0-rings

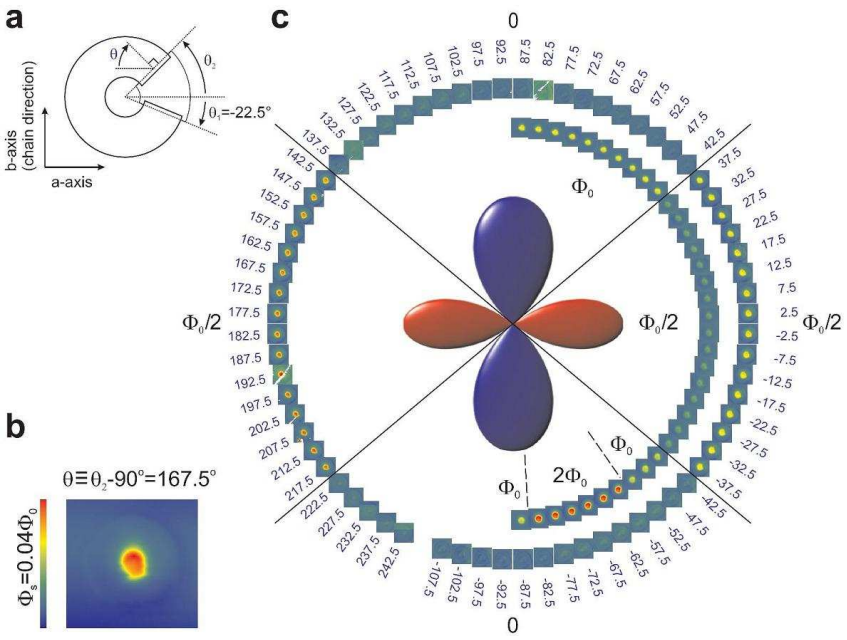

Figure 6. (color) (a) Schematic of one ring, with the angles defined. (b) An image of the ring with second junction normal angle $\theta = 167.5°$ relative to the majority twin a-axis direction, cooled and imaged in nominally zero field. (c) Images for all of the rings labelled by θ and arranged in a polar plot. Rings cooled in zero field were either in the $n = 0$ or the $n = 1/2$ flux quantum states (outer circle); the rings cooled in 0.2 μT were in the $n = 1/2$, $n = 1$ or $n = 2$ states (inner circle) [from (Kirtley et al., 2006)].

and π-rings occurring at angle of the variable junction normal θ values close to $(2m + 1)45°$, m being an integer. The deviations from four-fold symmetry are systematic and are consistent with the gap being larger in the *b*-axis direction than in the *a*-axis direction. The outer circle of images are of the sample cooled in zero field, in which case the rings either have zero spontaneous flux (fluxoid number $n = 0$) or spontaneous flux close to $\Phi_0/2$ ($n = 1/2$). To test whether all of the rings had sufficiently large junction critical currents to sustain an appreciable circulating supercurrent, we recooled the sample in a field of 0.2 μT, with the resulting images shown in the inner semi-circle of Fig. 6c. In this case the 0-rings were either in the $n = 1$ or 2 state, whereas the π-rings remained in the $n = 1/2$ state. This shows that the nodal direction in YBCO films with a predominant twin orientation is shifted by at least a few degrees from the $(2m + 1)45°$ angles expected for a pure $d_{x^2-y^2}$ superconductor. Furthermore, the spontaneous fluxes which do not deviate from $\Phi_0/2$ or zero underline the fact that BTRS is not associated with high temperature superconductivity in optimally doped YBCO.

4. Coupling of half-flux quanta

Using grain boundary junctions, it has only been possible to controllably generate individual π-ring (Tsuei et al., 1994; Tsuei and Kirtley, 2000a). Such ring has a doubly degenerate ground state in zero applied flux. This is of interest as model systems for studying magnetic phenomena −including frustration effects− in Ising antiferromagnets (Aeppli and Chandra, 1997; Moessner and Sondhi, 2001; Chandra and Doucot, 1988; Davidovic et al., 1996; Pannetier et al., 1984; Lerch et al., 1990). Furthermore, studies of coupled π-loops can be useful for designing quantum computers based on flux-qubits (Mooij et al., 1999; van der Wal et al., 2000; Friedman et al., 2000; Ioffe et al., 1999; Blais and Zagoskin, 2000) with viable quantum error correction capabilities (Preskill, 1998; Bennet and DiVincenzo, 2000). However, these require a large number of rings. In this section we concentrate on the realization of large-scale coupled π-loop arrays based on YBCO/Nb Josephson contacts. Scanning SQUID microscopy (Kirtley et al., 1995b; Kirtley et al., 1995a) has been used to study the ordering of half-flux quanta in these structures.

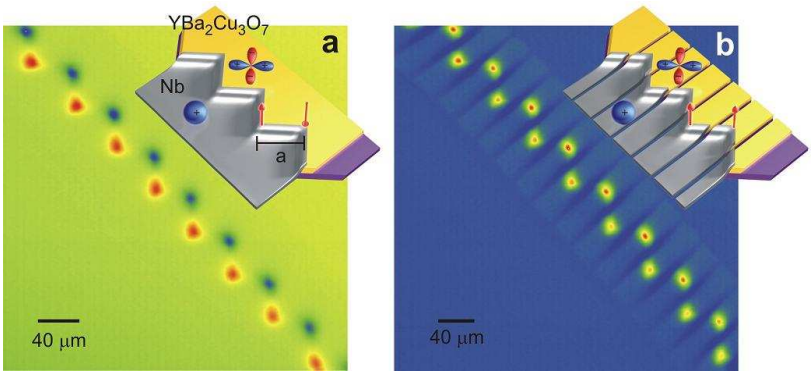

Figure 7. (color) Scanning SQUID microscope images of (a) continous zigzag junction with 40 μm facet lengths, and (b) electrically disconnected zigzag junction with 40 μm between facet corners [from (Hilgenkamp et al., 2003)].

We have first investigated the generation and coupling of half-integer flux quanta in the zigzag array that have been discussed in Sec. 3.2, shown schematically in Fig 7 insets. In the scanning SQUID microscopy image presented in Fig. 7a, a spontaneously induced magnetic flux is clearly seen at every corner of the zigzag structure. For this sample $a = 40$ μm, which implies that the facets are well within the wide limit. The observed corner fluxons are arranged in an antiferromagnetic fashion. This antiferromagnetic ordering was found to be very robust, occurring for many cool-downs and for different samples with comparable geometries. Deviations from an antiferromagnetic arrangement were only observed when

a magnetic field was applied during cool-down, or when an Abrikosov vortex was found trapped in (or near) the junction interface.

In the zigzag configuration, all the half-fluxons are generated in a singly connected superconducting structure; the question therefore arises as to whether the antiferromagnetic ordering is due to a magnetic interaction between the fractional fluxons, or to an interaction via the superconducting connection between the corners. To investigate this, we have also fabricated arrays of corner junctions, in a similar configuration as the zigzag arrays but with 2.5 μm-wide slits etched halfway between the corners, as schematically shown in Fig. 7b inset. In this situation there is no superconducting connection between the separate flux-generating corner junctions. For a distance between the corners equal to the facet length in the connected array, $a = 40$ μm, a ferromagnetic arrangement of the fractional flux quanta was observed (Fig. 7b). The magnetic interaction between the half-flux quanta at these distances is expected to be very weak, and alignment along minute spurious background fields in the scanning SQUID microscope is anticipated to be the dominating mechanism for their parallel arrangement. When the distance was decreased to about 20 μm, with a slit width of 1.5 μm, a tendency towards an antiferromagnetic coupling was observed.

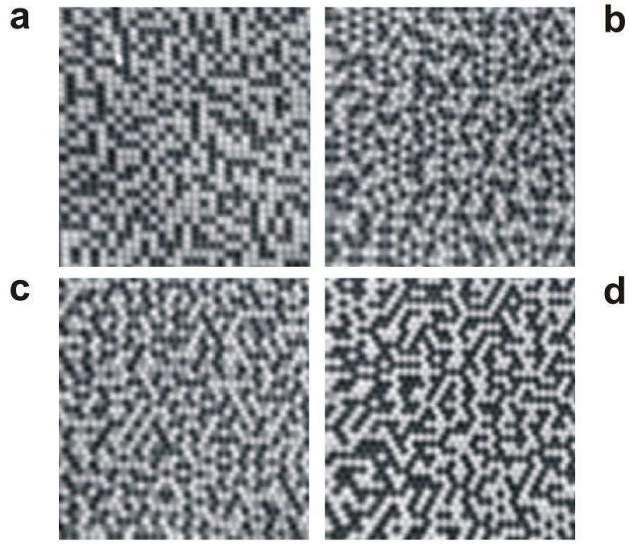

Figure 8. SQUID microscopy images of four electrically disconnected arrays of π-rings with 2.7 μm junctions and 11.5 μm ring to ring spacings for (a) square, (b) honeycomb, (c) kagomé, and (d) triangle lattices [from (Kirtley et al., 2005)].

We also have investigated 2-dimensional π-ring arrays made up of individual rings with various nearest-neighbor distances (25 μm or closer) (Hilgenkamp et al., 2003; Kirtley et al., 2005). The rings were arranged into arrays with 4

different geometries: square, honeycomb, triangular, and kagomé. The square and honeycomb arrays are geometrically unfrustrated, as their magnetic moments can be arranged so that all nearest neighbors have opposite spins, and the ground state of these lattices are only doubly degenerate. In contrast, the triangle and kagomé lattices are geometrically frustrated, since it is impossible for all of the rings to have all nearest neighbors anti-ferromagnetically aligned, and the ground states are highly degenerate. Figure 8 shows examples of scanning SQUID microscope images of the arrays after cooling in nominally zero field. Although regions of antiferromagnetic ordering are seen in the unfrustrated arrays Figs. 8a and 8b, anti-ferromagnetic ordering beyond a few lattice distances was never observed. Nevertheless, antiferromagnetic correlations were seen in all the 2D π-ring arrays.

We have shown that it is possible to realize large arrays of photolithographically patterned π-rings. Half-fluxon Josephson vortices in electrically connected zigzag junctions order with strongly anti-parallel half-fluxon vortices through the superconducting order parameter phase. Electrically isolated 1D and 2D arrays order much less strongly. The 2D π-ring arrays show stronger anti-ferromagnetic correlations than reported previously for 0-ring arrays (Davidovic et al., 1997; Davidovic et al., 1996), but do not order beyond a few lattice constants. One possibility is that our arrays correspond to a spin glass (Kirtley et al., 2005). However, in the absence of some hidden symmetry breaking, it appears that our rings are simply doubly degenerate. Furthermore, qualitatively similar results are obtained for arrays with and without geometrical frustration. Our experiments with repeated cooling show that there is little fixed disorder in our arrays. Therefore, it seems unlikely that we have a spin glass, unless there is some form of frozen-in disorder that varies from cooldown to cooldown.

5. Possible applications of π-phase-shifting elements

Besides holding a clue to the mechanism of high-T_c superconductivity, the unconventional *d*-wave symmetry in high-T_c cuprates provides unique possibilities to realize superconducting (quantum)-electronics that exploit the associated sign-changes in the order parameter for orthogonal directions in *k*-space. An intriguing consequence of this sign-change is the spontaneous generation of fractional magnetic flux quanta in superconducting rings incorporating a *d*-wave induced π-phase shift. In the following, we discuss some possible applications of π-phase-shifting elements for novel (quantum)-electronics based on high-T_c versus low-T_c Josephson contacts.

5.1. COMPLEMENTARY JOSEPHSON ELECTRONICS

For a built-in phase shift of $k\pi$, the $I_c(B)$ characteristics of π-SQUIDs are shifted by $\frac{1}{2}k\Phi_0$ compared to a standard SQUID. Two $I_c(B)$ dependencies are possible,

differing with the polarity of the built-in phase shift. By constructing a phase-shifting element in which the polarity can be switched, a bistable superconducting device can be realized, with SQUID characteristics shifted by $+\frac{1}{2}k\Phi_0$ or $-\frac{1}{2}k\Phi_0$ compared to the standard case. This bistability can be used to construct superconducting memory elements, like flip-flops or programmable logic. Furthermore, Ioffe et al. (1999) proposed to design qubits for quantum computation based on the energetically degenerate ground states. They suggested a possible practical realization with $k = \pm\frac{1}{2}$ (Fig. 9a). It is based on a superconducting ring containing four identical Josephson junctions. In this ring a $\pi-$phase shift is incorporated using one of the concepts described earlier. It invokes a persistent circulating supercurrent I_{circ} relating to a phase drop of practically $\frac{1}{4}\pi$ per junction, with a slight deviation proportional to the magnetic flux in the ring, which is equal to the product of I_{circ} and the inductance of the phase-shifting element $L_{shifter}$.

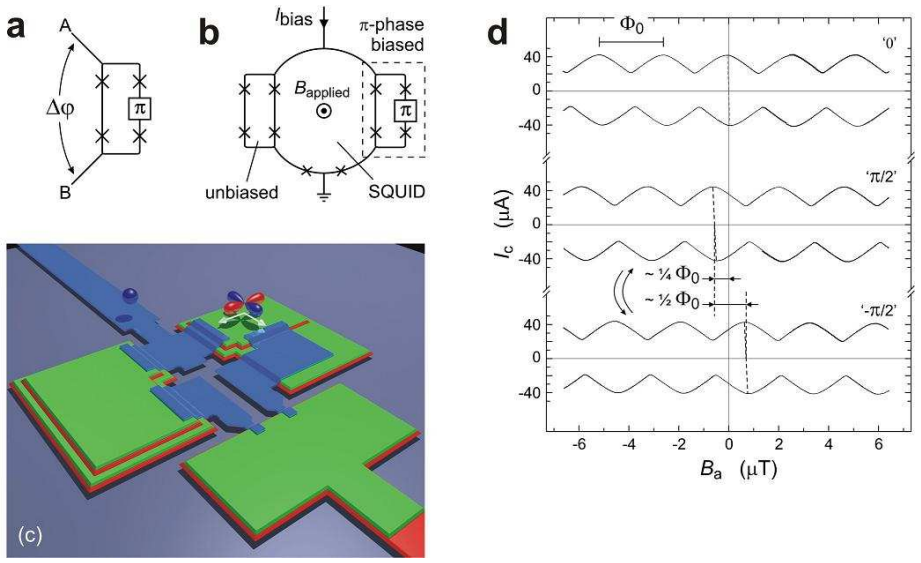

Figure 9. (Color) Schematic of (a) a $\pi/2$ phase-shifting element consisting of four Josephson junctions and a built-in π phase shift, and (b) a switchable $\pi/2$ SQUID, in which a SQUID loop incorporates the $\pi/2$ phase shifter (dashed rectangle) and an unbiased four-junction loop. (c) Implementation of the switchable $\pi/2$ SQUID. (d) Critical current versus applied magnetic field for a reference SQUID incorporating two unbiased four-junction loops (top), and for the two complementary states of the switchable $\pi/2$ SQUID (middle and bottom) [from (Smilde et al., 2004b)].

We have realized a superconducting bistable device by incorporating a $\pi/2$ phase-shifting element into a dc SQUID. Incorporating this element in a larger SQUID structure, as shown in Fig. 9b, a phase shift over the terminals A and B of $\pm\pi/2$ is obtained whose polarity depends on the direction of I_{circ}. With the I_c's of the junctions in the overall SQUID being much smaller than those in the phase

shifter, the final device is bistable, with the $I_c(B)$ characteristics shifted by $+\frac{1}{4}\Phi_0$ or $-\frac{1}{4}\Phi_0$ compared to a standard SQUID, as shown in Fig. 9d. Notice that the characteristics of these two states are complementary to each other, which makes these structures suitable for the construction of (programmable) complementary Josephon electronics.

5.2. HALF-FLUX QUANTA AS INFORMATION CARRIERS

The doubly degenerate groundstates of π-rings allow their use for information storage. As previously discussed, under specific circumstances these groundstates are characterized by the spontaneous formation of half a quantum of magnetic flux. Their polarity can be set by the action of a logic (quantum-)gate, making them potentially useful elements for a random access memory. This is demonstrated in Fig. 10, showing a scanning SQUID microscopy image of an array of half-integer flux quanta forming the characters 'IBM+UT'. The fluxes were all set to have the same polarity by cooling in a modest externally applied magnetic field. The polarity of selected elements was reversed by applying pulses of control current to a single turn coil incorporated into the SQUID measurement chip.

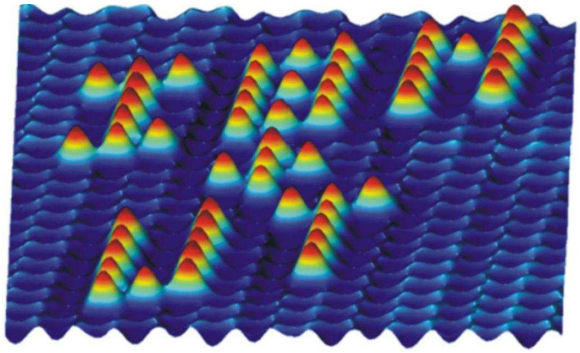

Figure 10. Scanning SQUID microscopy image of an array of half-integer flux quanta forming the characters 'IBM+UT'.

5.3. π-SHIFTS IN RAPID SINGLE FLUX QUANTUM-LOGIC

In isolated π-rings, fabricated with high-T_c grain boundaries (Tsuei et al., 1994) or with connections between high-T_c and low-T_c superconductors (Hilgenkamp et al., 2003), the generation and manipulation of fractional flux quanta has already been demonstrated using scanning SQUID microscopy. An important step towards its application in electronic circuitry is the incorporation of such π-loops in superconducting logic gates, in which a controlled operation on an electronically applied input signal leads to a predefined output signal (Terzioglu and Beasley,

1998; Ustinov and Kaplunenko, 2003). We have performed experiments realizing this idea (Ortlepp et al., 2006), and showed the first realization of a Toggle Flip-Flop (TFF) based on Josephson contacts between high-T_c and low-T_c superconductors, in which the polarity of the fractional flux quantum provides the internal memory.

The spontaneous generation of fractional flux in the π-shift device eliminates the need for the asymmetrically injected bias current, which reduces the amount of connections to external control-electronics and allows for symmetry in the design parameters. This greatly benefits the design-process and fabrication and also leads to denser circuitry; our first realization needed only a quarter of the size of a standard Toggle Flip-Flop in established Niobium technology with the same feature size of 2.5 μm.

5.4. π-SHIFT QUBIT CONCEPTS

Over the last decades quantum-computation has received much attention because of its potential to solve mathematical problems, which classical computers cannot solve in acceptable times (DiVincenzo, 1995; DiVincenzo and Loss, 1998). As usual, it is a long way from basic principles to their practical implementation. A central aspect in this context is the availability of appropriate qubit elements, which allow integration into logic gates. A qubit is a quantum-system which, similar to a bit in a conventional computer, is characterized by two states but which can exist in arbitrary quantum-superpositions of these states.

While techniques from quantum-optics (cold trapped atoms, photons in cavities) or from molecular physics (nuclear magnetic resonance methods) appear to provide promising technologies for the realization of individual and few qubits, freedom in the design-parameters of the qubits and upscaling to real computing devices will require the scalability and variability of solid-state implementations. Superconductors appear to provide the best starting point to achieve this goal.

Proposed superconducting qubits operate either with charge (Schnirman et al., 1997; Averin, 1998; Bouchiat et al., 1998; Nakamura et al., 1999), or flux-/phase-states (Bocko et al., 1997; Mooij et al., 1999; Ioffe et al., 1999; Feigel'man et al., 2000; Blatter et al., 2001). In the phase-qubit, the information is mainly expressed through the phase degree of freedom, with only a minor coupling to the environment or to other qubits. The phase-state itself carries no charge and no current, rendering the device electrically and magnetically robust. A first proposal that was made by the ETH Zürich group for a superconducting phase-qubit involved mesoscopic junctions combining *s*- and *d*-wave superconductors, so called SDS'-junctions (Ioffe et al., 1999). Subsequently, a more easily realizable scheme was proposed involving superconducting loops with five Josephson junctions, four conventional ones and a π-junction (Blatter et al., 2001). In the design, the quantum degrees of freedom involve only the conventional junctions, while π-junction

acts primarily as a phase-shifter. A very appealing aspect hereby is the fact that the qubits do not require a flux-bias, as is the case for all-low-T_c concepts.

Acknowledgements

We would like to thank A. Brinkman, M. Dekkers, A. Golubov, S. Harkema, T. Ortlepp, and F. Roesthuis for discussions. This work was supported by the Dutch Foundation for Research on Matter (FOM), the Netherlands Organization for Scientific Research (NWO), the Dutch STW NanoNed programme, and the European Science Foundation (ESF) PiShift programme.

References

Aeppli, G. and Chandra, P. (1997) Seeking a simple complex system, *Science* **275**, 177.

Akoh, H., Camerlingo, C., and Takada, S. (1990) Anisotropic Josephson junctions of Y-Ba-Cu-O/Au/Nb film sandwiches, *Appl. Phys. Lett.* **56**, 1487.

Akoh, H., Shinoki, F., Takahashi, M., and Takada, S. (1988) S-N-S Josephson junction consisting of Y-Ba-Cu-O/Au/Nb thin-films, *Jpn. J. Appl. Phys.* **27**, L519.

Akoh, H., Shinoki, F., Takahashi, M., and Takada, S. (1989) Fabrication of S-N-S Josephson-junctions of Y-Ba-Cu-O/Au/Nb sandwices, *IEEE Trans. Magn.* **25**, 795.

Ariando, Darminto, D., Smilde, H.-J., Rogalla, H., and Hilgenkamp, H. (2005) Phase-sensitive order parameter symmetry test experiments utilizing $Nd_{2-x}Ce_xCuO_{4-y}$/Nb zigzag junctions, *Phys. Rev. Lett.* **94**, 167001.

Averin, D. V. (1998) Adiabatic quantum computation with Cooper pairs, *Sol. State Commun.* **105**, 659.

Balci, H. and Greene, R. L. (2004) Anomalous change in the field dependence of the electronic specific heat of an electron-doped cuprate superconductor, *Phys. Rev. Lett.* **93**, 067001.

Basov, D. N., Liang, R., Bonn, D. A., Hardy, W. N., Dabrowski, B., Quijada, M., Tanner, D. B., Rice, J. P., Ginsberg, D. M., and Timusk, T. (1995) In-plane anisotropy of the penetration depth in $YBa_2Cu_3O_{7-x}$ and $YBa_2Cu_4O_8$ superconductors, *Phys. Rev. Lett.* **74**, 598.

Beasley, M. R., Lew, D., and Laughlin, R. B. (1994) Time-reversal symmetry breaking in superconductors: a proposed experimental test, *Phys. Rev. B* **49**, 12330.

Bennet, C. H. and DiVincenzo, D. P. (2000) Quantum information and computation, *Nature* **404**, 247.

Biswas, A., Fournier, P., Qazilbash, M. M., Smolyaninova, V. N., Balci, H., and Greene, R. L. (2002) Evidence of a $d-$ to s-wave pairing symmetry transition in the electron-doped cuprate superconductor $Pr_{2-x}Ce_xCuO_4$, *Phys. Rev. Lett.* **88**, 207004.

Blais, A. and Zagoskin, A. M. (2000) Operation of universal gates in a solid-state quantum computer based on clean Josephson junctions between d-wave superconductors, *Phys. Rev. A* **61**, 042308.

Blank, D. H. A. and Rogalla, H. (1997) Effect of ion milling on the morphology of ramp-type Josephson junctions, *J. Mater. Res.* **12**, 2952.

Blatter, G., Geshkenbein, V. B., and Ioffe, L. B. (2001) Design aspects of superconducting-phase quantum bits, *Phys. Rev. B* **63**, 174511.

Bocko, M. F., Herr, A. M., and Feldman, M. J. (1997) Prospects for quantum coherent computation using superconducting electronics, *IEEE Trans. Appl. Supercond.* **7**, 3638.

Bouchiat, V., Vion, D., Joyez, P., Esteve, D., and Devoret, M. H. (1998) Quantum coherence with a single Cooper pair, *Physica Scripta* **T76**, 165.

Brawner, D. A. and Ott, H. R. (1994)a Evidence for an unconventional superconducting order-parameter in $YBa_2Cu_3O_6.9$, *Phys. Rev. B* **50**, 6530.

Brawner, D. A. and Ott, H. R. (1994)b Evidence for unconventional superconductivity in $YBa_2Cu_3O_6.9$, *Physica C* **235**, 1867.

Brawner, D. A. and Ott, H. R. (1996) Evidence for a non-*s*-wave superconducting order parameter in $YBa_2Cu_3O_6.6$ with $T_c = 60$ K, *Phys. Rev. B* **53**, 8249.

Bulaevskii, L. N., Kuzii, V. V., and Sobyanin, A. A. (1977) Superconducting system with weak coupling to current in ground-state, *JETP Lett.* **25**, 290.

Chandra, P. and Doucot, B. (1988) Possible spin-liquid state at large S for the frustrated square Heisenberg lattice, *Phys. Rev. B* **38**, 9335.

Chesca, B., Doenitz, D., Dahm, T., Huebener, R. P., Koelle, D., Kleiner, R., Ariando, Smilde, H. J. H., and Hilgenkamp, H. (2006) Observation of Andreev bound states in $YBa_2Cu_3O_{7-x}$/Au/Nb ramp-type Josephson junctions, *Phys. Rev. B* **73**, 014529.

Chesca, B., Ehrhardt, K., Mossle, M., Straub, R., Koelle, D., Kleiner, R., and Tsukada, A. (2003) Magnetic-field dependence of the maximum supercurrent of $La_{2-x}Ce_xCuO_{4-y}$ interferometers: Evidence for a predominant $d_{x^2-y^2}$ superconducting order parameter, *Phys. Rev. Lett.* **90**, 057004.

Chesca, B., Seifried, M., Dahm, T., Schopohl, N., Koelle, D., Kleiner, R., and Tsukada, A. (2005) Observation of Andreev bound states in bicrystal grain-boundary Josephson junctions of the electron-doped superconductor $La_{2x}Ce_xCuO_{4y}$, *Phys. Rev. B* **71**, 104504.

Copetti, C. A., Rüders, F., Oelze, B., Buchal, C., Kabius, B., and Seo, J. W. (1995) Electrical-properties of 45° grain-boundaries of epitaxial YBaCuO, dominated by crystalline microstructure and *d*-wave-symmetry, *Physica C* **253**, 63.

Covington, M., Aprili, M., Paraoanu, E., , Greene, L. H., Xu, F., Zhu, J., , and Mirkin, C. A. (1997) Observation of surface-induced broken time-reversal symmetry in $YBa_2Cu_3O_7$ tunnel junctions, *Phys. Rev. Lett.* **79**, 277.

Dagan, Y. and Deutscher, G. (2001) Doping and magnetic field dependence of in-plane tunneling into $YBa_2Cu_3O_{7-x}$: possible evidence for the existence of a quantum critical point, *Phys. Rev. Lett.* **87**, 177004.

Davidovic, D., Kumar, S., Reich, D. H., Siegel, J., Field, S. B., Tiberio, R. C., Hey, R., and Ploog, K. (1996) Magnetic correlations, geometrical frustration, and tunable disorder in arrays of superconducting rings, *Phys. Rev. B* **55**, 6518.

Davidovic, D., Kumar, S., Reich, D. H., Siegel, J., Field, S. B., Tiberio, R. C., Hey, R., and Ploog, K. (1997) Correlations and disorder in arrays of magnetically coupled superconducting rings, *Phys. Rev. Lett.* **76**, 815.

DiVincenzo, D. P. (1995) Quantum Computation, *Science.* **270**, 255.

DiVincenzo, D. P. and Loss, D. (1998) Quantum computation is physical, *Superlattices Microstruct.* **23**, 419.

Engelhardt, A., Dittmann, R., and Braginski, A. I. (1999) Subgap conductance features of $YBa_2Cu_3O_{7-\delta}$ edge Josephson junctions, *Phys. Rev. B* **59**, 3815.

Fauque, B., Sidis, Y., Hinkov, V., Pailhes, S., Lin, C., Chaud, X., and Bourges, P. (2005) Magnetic order in the pseudogap phase of high-T_c superconductors, *Preprint at http://arxiv.org/abs/cond-mat/0509210.*

Feigel'man, M. V., Ioffe, L. B., Geshkenbein, V. B., and Blatter, G. (2000) Andreev spectroscopy for superconducting phase qubits, *J. Low Temp. Phys.* **118**, 805.

Foote, M. C., Hunt, B. D., and Bajuk, L. J. (1991) $YBa_2Cu_3O_{7-\delta}$/Au/Nb sandwich geometry SNS weak links on *c*-axis oriented $YBa_2Cu_3O_{7-\delta}$, *IEEE Trans. Magn.* **27**, 1335.

Friedman, J. R., Patel, V., Chen, W., Tolpygo, S. K., and Lukens, J. E. (2000) Quantum superposition of distinct macroscopic states, *Nature* **406**, 43.

Fujimaki, A., Takai, Y., and Hayakawa, H. (1991) Experimental-analysis of superconducting properties of Y-Ba-Cu-O/Ag proximity interfaces, *IEEE Trans. Magn.* **27**, 1353.

Fujimaki, A., Tamaoki, T., Hidaka, T., Yanagase, M., Shiota, T., Takai, Y., and Hayakawa, H. (1990) Experimental-analysis of $YBa_2Cu_3O_x$/Ag proximity interfaces, *Jpn. J. Appl. Phys.* **29**, L1659.

Gao, J., Aarnink, W. A. M., Gerritsma, G. J., and Rogalla, H. (1990) Controlled preparation of all high-T_c SNS-type edge junctions and dc squids, *Physica C* **171**, 126.

Gao, J., Boguslavskij, Y., Klopman, B. B. G., Terpstra, D., Gerritsma, G. J., and Rogalla, H. (1991) Characteristics of advanced $YBa_2Cu_3O_x$ $PrBa_2Cu_3O_x$ $YBa_2Cu_3O_x$ edge type junctions, *Appl. Phys. Lett.* **59**, 2754.

Geshkenbein, V. B. and Larkin, A. I. (1986) The Josephson effect in superconductors with heavy fermions, *JETP Lett.* **43**, 395.

Geshkenbein, V. B., Larkin, A. I., and Barone, A. (1987) Vortices with half magnetic flux quanta in heavy-fermion superconductors, *Phys. Rev. B* **36**, 235.

Gim, Y., Mathai, A., Black, R. C., Amar, A., and Wellstood, F. C. (1996) Symmetry of the phase of the order parameter in $YBa_2Cu_3O_{7-\delta}$, *Journal de Physique I* **6**, 2299.

Goldobin, E., Sterck, A., Gaber, T., Koelle, D., and Kleiner, R. (2004) Dynamics of semifluxons in Nb long Josephson 0-π junctions, *Phys. Rev. Lett.* **92**, 057005.

Golubov, A. A., Kupriyanov, M. Y., and Il'ichev, E. (2004) The current-phase relation in Josephson junctions, *Rev. Mod. Phys.* **76**, 411.

Hilgenkamp, H., Ariando, Smilde, H. J. H., Blank, D. H. A., Rijnders, G., Rogalla, H., Kirtley, J. R., and Tsuei, C. C. (2003) Ordering and manipulation of the magnetic moments in large-scale superconducting π-loop arrays, *Nature* **422**, 50.

Hilgenkamp, H. and Mannhart, J. (2002) Grain boundaries in high-T_c superconductors, *Rev. Mod. Phys.* **74**, 485.

Hilgenkamp, H., Mannhart, J., and Mayer, B. (1996) Implications of $d_{x^2-y^2}$ symmetry and faceting for the transport properties of grain boundaries in high-T_c superconductors, *Phys. Rev. B* **53**, 14586.

Hu, C. R. (1994) Midgap surface states as a novel signature for $d_{x^2-y^2}$-wave superconductivity, *Phys. Rev. Lett.* **72**, 1526.

Hunt, B. D., Foote, M. C., and Bajuk, L. J. (1991) Edge-geometry $YBa_2Cu_3O_{7-x}$/Au/Nb SNS devices, *IEEE Trans. Magn.* **27**, 848.

Hunt, B. D., Foote, M. C., and Vasquez, R. P. (1990) Electrical characterization of chemically modified $YBa_2Cu_3O_{7-x}$ surfaces, *Appl. Phys. Lett.* **56**, 2678.

Ioffe, L. B., Geshkenbein, V. B., Feigel'man, M. V., Fauchere, A. L., and Blatter, G. (1999) Environmentally decoupled *sds*-wave Josephson junctions for quantum computing, *Nature* **398**, 679.

Kaminski, A., Rosenkranz, S., Fretwell, H. M., Campuzano, J. C., Li, Z., Raffy, H., Cullen, W. G., You, H., Olson, C. G., Varma, C. M., and Hochst, H. (2002) Spontaneous breaking of time reversal symmetry in the pseudogap state of a high-T_c superconductor, *Nature* **416**, 610.

Kashiwaya, S. and Tanaka, Y. (2000) Tunnelling effects on surface bound states in unconventional superconductors, *Rep. Prog. Phys.* **63**, 1641.

Kirtley, J. R., Ketchen, M. B., Stawiasz, K. G., Sun, J. Z., Gallagher, W. J., Blanton, S. H., and Wind, S. J. (1995)a High-resolution scanning SQUID microscope, *Appl. Phys. Lett.* **66**, 1138.

Kirtley, J. R., Ketchen, M. B., Tsuei, C. C., Sun, J. Z., Gallagher, W. J., Yu-Jahnes, L. S., Gupta, A., Stawiasz, K. G., and Wind, S. J. (1995)b Design and applications of a scanning SQUID microscope, *IBM J. Res. Develop.* **39**, 655.

Kirtley, J. R., Moler, K. A., and Scalapino, D. J. (1997) Spontaneous flux and magnetic-interference patterns in 0-π Josephson junctions, *Phys. Rev. B* **56**, 886.

Kirtley, J. R., Tsuei, C. C., Ariando, Smilde, H. J. H., and Hilgenkamp, H. (2005) Antiferromagnetic ordering in arrays of superconducting π-rings, *Phys. Rev. B* **72**, 214521.

Kirtley, J. R., Tsuei, C. C., Ariando, A., Verwijs, C. J. M., Harkema, S., and Hilgenkamp, H. (2006) Angle-resolved phase-sensitive determination of the in-plane gap symmetry in $YBa_2Cu_3O_{7-\delta}$, *Nature Physics*.

Laughlin, R. B. (1988) The relationship between high-temperature superconductivity and the fractional quantum hall effect, *Science* **242**, 525.

Lawrence, T. W., Szoker, A., and Laughlin, R. B. (1992) Absence of circular dichroism in high-temperature superconductors, *Phys. Rev. Lett.* **69**, 1439.

Lerch, P., Leemann, C., Theron, R., and Martinoli, P. (1990) Dynamics of the phase-transition in proximity-effect arrays of Josephson-junctions at full frustration, *Phys. Rev. B* **41**, 11579.

Lofwander, T., Shumeiko, V. S., and Wendin, G. (2001) Andreev bound states in high-T_c superconducting junctions, *Supercond. Sci. Technol.* **14**, R53.

Lu, D. H., Feng, D. L., Armitage, N. P., Shen, K. M., Damascelli, A., Kim, C., Ronning, F., Bonn, D. A., Liang, R., Hardy, W. N., Rykov, A. I., and Tajima, S. (2001) Superconducting gap and strong in-plane anisotropy in untwinned $YBa_2Cu_3O_{7-\delta}$, *Phys. Rev. Lett.* **86**, 4370.

Majer, J. B., Butcher, J. R., and Mooij, J. E. (2002) Simple phase bias for superconducting circuits, *Appl. Phys. Lett.* **80**, 3638.

Mannhart, J., Mayer, B., and Hilgenkamp, H. (1996) Anomalous dependence of the critical current of 45° grain boundaries in $YBa_2Cu_3O_{7-x}$ on an applied magnetic field, *Z. Phys. B* **101**, 175.

Mathai, A., Gim, Y., Black, R. C., Amar, A., and Wellstood, F. C. (1995) Experimental proof of a time-reversal-invariant order parameter with a π shift in $YBa_2Cu_3O_{7-\delta}$, *Phys. Rev. Lett.* **74**, 4523.

Mints, R. G. and Kogan, V. G. (1997) Josephson junctions with alternating critical current density, *Phys. Rev. B* **55**, R8682.

Mints, R. G., Papiashvili, I., Kirtley, J. R., Hilgenkamp, H., Hammerl, G., and Mannhart, J. (2002) Observation of splintered Josephson vortices at grain boundaries in $YBa_2Cu_3O_{7-\delta}$, *Phys. Rev. Lett.* **89**, 067004.

Moessner, R. and Sondhi, S. L. (2001) Ising models of quantum frustration, *Phys. Rev. B* **63**, 224401.

Mooij, J. E., Orlando, T. P., Levitov, L., Tian, L., van der Wal, C. H., and Lloyd, S. (1999) Josephson persistent-current qubit, *Science* **285**, 1036.

Nakamura, Y., Pashkin, Y. A., and Tsai, J. S. (1999) Coherent control of macroscopic quantum states in a single-Cooper-pair box, *Nature* **398**, 786.

Ng, T. K. and Varma, C. M. (2004) Experimental signatures of time-reversal-violating superconductors, *Phys. Rev. B* **70**, 054514.

Ortlepp, T., Ariando, Mielke, O., Verwijs, C. J. M., Foo, K. F. K., Rogalla, H., Uhlmann, F. H., and Hilgenkamp, H. (2006) Flip-flopping fractional flux quanta, *Science* **312**, 1495.

Pannetier, B., Chaussy, J., Rammal, R., and Villegier, J. C. (1984) Experimental fine tuning of frustration: Two-dimensional superconducting network in a magnetic Field, *Phys. Rev. Lett.* **53**, 1845.

Polturak, E., Koren, G., Cohen, D., and Aharoni, E. (1993) Measurements of the anisotropy and temperature dependence of the in-plane energy gap in $YBa_2Cu_3O_{7-\delta}$ using Andreev reflections, *Phys. Rev. B* **47**, 5270.

Preskill, J. (1998) Reliable quantum computers, *Proc. R. Soc. Lond. A* **454**, 385.

Qazilbash, M. M., Biswas, A., Dagan, Y., Ott, R. A., and Greene, R. L. (2003) Point-contact spectroscopy of the electron-doped cuprate superconductor $Pr_{2x}Ce_xCuO_4$: The dependence of conductance-voltage spectra on cerium doping, barrier strength, and magnetic field, *Phys. Rev. B* **68**, 024502.

Rykov, M. F. L. A. I. and Tajima, S. (1998) Raman scattering study on fully oxygenated $YBa_2Cu_3O_7$ single crystals: *xy* anisotropy in the superconductivity-induced effects, *Phys. Rev. Lett.* **80**, 825.

Schnirman, A., Schon, G., and Hermon, Z. (1997) Quantum manipulations of small Josephson junctions, *Phys. Rev. Lett.* **79**, 2371.

Schulz, R. R., Chesca, B., Goetz, B., Schneider, C. W., Schmehl, A., Bielefeldt, H., Hilgenkamp, H., Mannhart, J., and Tsuei, C. C. (2000) Design and realization of an all *d*-wave dc π-superconducting quantum interference device, *Appl. Phys. Lett.* **76**, 912.

Sharoni, A., Millo, O., Kohen, A., Dagan, Y., Beck, R., Deutscher, G., and Koren, G. (2002) Local and macroscopic tunneling spectroscopy of $Y_{1-x}Ca_xBa_2Cu_3O_{7-d}$ films: evidence for a doping-dependent *is* or *idxy* component in the order parameter, *Phys. Rev. B* **65**, 134526.

Sigrist, M. (1998) Time-reversal symmetry breaking states in high-temperature superconductors, *Prog. Theor. Phys.* **99**, 899.

Sigrist, M. and Rice, T. M. (1992) Paramagnetic effect in high-T_c superconductors - a hint for *d*-wave superconductivity, *J. Phys. Soc. Jpn.* **61**, 4283.

Skinta, J. A., Kim, M. S., Lemberger, T. R., Greibe, T., and Naito, M. (2002) Evidence for a transition in the pairing symmetry of the electron-doped cuprates $La_{2x}Ce_xCuO_{4y}$ and $Pr_{2x}Ce_xCuO_{4y}$, *Phys. Rev. Lett.* **88**, 207005.

Smilde, H. J. H., Ariando, Blank, D. H. A., Gerritsma, G. J., Hilgenkamp, H., and Rogalla, H. (2002)a *d*-waveinduced Josephson current counterflow in $YBa_2Cu_3O_7$/Nb Zigzag Junctions, *Phys. Rev. Lett.* **88**, 057004.

Smilde, H. J. H., Ariando, Blank, D. H. A., Hilgenkamp, H., and Rogalla, H. (2004)a π-SQUIDs based on Josephson contacts between high-T_c and low-T_c superconductors, *Phys. Rev. B* **70**, 024519.

Smilde, H. J. H., Ariando, Rogalla, H., and Hilgenkamp, H. (2004)b Bistable superconducting quantum interference device with built-in switchable $\pi/2$ phase shift, *Appl. Phys. Lett.* **85**, 4091.

Smilde, H. J. H., Golubov, A. A., Ariando, Rijnders, G., Dekkers, J. M., Harkema, S., Blank, D. H. A., Rogalla, H., and Hilgenkamp, H. (2005) Admixtures to *d*-wave gap symmetry in untwinned $YBa_2Cu_3O_7$ superconducting films measured by angle-resolved electron tunneling, *Phys. Rev. Lett.* **95**, 257001.

Smilde, H. J. H., Hilgenkamp, H., Gerritsma, G. J., Blank, D. H. A., and Rogalla, H. (2001)a Realization and properties of ramp-type $YBa_2Cu_3O_{7-\delta}$/Au/Nb junctions, *Physica C* **350**, 269.

Smilde, H. J. H., Hilgenkamp, H., Gerritsma, G. J., Blank, D. H. A., and Rogalla, H. (2001)b Y-Ba-Cu-O/Au/Nb ramp-type Josephson junctions, *IEEE Trans. Appl. Supercond.* **11**, 501.

Smilde, H. J. H., Hilgenkamp, H., Rijnders, G., Rogalla, H., and Blank, D. H. A. (2002)b Enhanced transparency ramp-type Josephson contacts through interlayer deposition, *Appl. Phys. Lett.* **80**, 4579.

Spielman, S., Dodge, J. S., Lombardo, L. W., Eom, C. B., Fejer, M. M., Geballe, T. H., and Kapitulnik, A. (1992) Measurement of the spontaneous polar Kerr effect in $YBa_2Cu_3O_7$ and $Bi_2Sr_2CaCu_2O_8$, *Phys. Rev. Lett.* **68**, 3472.

Tafuri, F. and Kirtley, J. R. (2005) Weak links in high critical temperature superconductors, *Rep. Prog. Phys.* **68**, 2573.

Terai, H., Fujimaki, A., Takai, Y., and Hayakawa, H. (1993) Magnetic-field dependence of high J_c $YBa_2Cu_3O_{7-x}$/Au/Nb junctions using alpha-axis-oriented $YBa_2Cu_3O_{7-x}$ thin-films, *Jpn. J. Appl. Phys.* **32**, L901.

Terai, H., Fujimaki, A., Takai, Y., and Hayakawa, H. (1995) Electrical interface structure $YBa_2Cu_3O_{7-x}$ metal contact, *IEEE Trans. Appl. Supercond.* **5**, 2408.

Terzioglu, E. and Beasley, M. R. (1998) Complementary Josephson junction devices and circuits: A possible new approach to superconducting electronics, *IEEE Trans. Appl. Sup.* **8**, 48.

Tsuei, C. C. and Kirtley, J. R. (2000)a Pairing symmetry in cuprate superconductors, *Rev. Mod. Phys.* **72**, 969.

Tsuei, C. C. and Kirtley, J. R. (2000)b Phase-sensitive evidence for *d*-wave pairing symmetry in electron-doped cuprate superconductors, *Phys. Rev. Lett.* **85**, 182.

Tsuei, C. C., Kirtley, J. R., Chi, C. C., Yu-jahnes, L. S., Gupta, A., Shaw, T., Sun, J. Z., and Ketchen, M. B. (1994) Pairing symmetry and flux quantization in a tricrystal superconducting ring of $YBa_2Cu_3O_{7-\delta}$, *Phys. Rev. Lett.* **73**, 593.

Tsuei, C. C., Kirtley, J. R., Hammerl, G., Mannhart, J., Raffy, H., and Li, Z. Z. (2004) Robust $d_{x^2y^2}$ pairing symmetry in hole-doped cuprate superconductors, *Phys. Rev. Lett.* **93**, 187004.

Usagawa, T., Wen, J. G., Ishimaru, Y., Koyama, S., Utagawa, T., and Enomoto, Y. (1998) Stability of ultrasmooth surface morphology of (110) $YBa_2Cu_3O_{7-\delta}$ homoepitaxial films and Nb/Au/(110) $YBa_2Cu_3O_{7-\delta}$ junctions, *Appl. Phys. Lett.* **72**, 3202.

Ustinov, A. V. and Kaplunenko, V. K. (2003) Rapid single-flux quantum logic using π-shifters, *J. Appl. Phys.* **94**, 5405.

van der Wal, C. H., ter Haar, A. C. J., Wilhelm, F. K., Schouten, R. N., and Mooij, C. J. P. M. H. T. P. O. S. L. J. E. (2000) Quantum superposition of macroscopic persistent-current states, *Science* **290**, 773.

van Harlingen, D. J. (1995) Phase-sensitive tests of the symmetry of the pairing state in the high-temperature superconductorsEvidence for $d_{x^2-y^2}$ symmetry, *Rev. Mod. Phys.* **67**, 515.

Varma, C. M. (1999) Pseudogap phase and the quantum-critical point in copper-oxide metals, *Phys. Rev. Lett.* **83**, 3538.

Varma, M. E. S. C. M. (2002) Detection and implications of a time-reversal breaking state in underdoped cuprates, *Phys. Rev. Lett.* **89**, 247003.

Verhoeven, M. A. J., Moerman, R., Bijlsma, M. E., Rijnders, A. J. H. M., Blank, D. H. A., Gerritsma, G. J., and Rogalla, H. (1996) Nucleation and growth of $PrBa_2Cu_3O_{7-\delta}$ barrier layers on ramps in $DyBa_2Cu_3O_{7-\delta}$ studied by atomic force microscopy, *Appl. Phys. Lett.* **68**, 1276.

Wen, J. G., Koshizuka, N., Tanaka, S., Satoh, T., Hidaka, M., and Tahara, S. (1999) Atomic structure and composition of the barrier in the modified interface high-T_c Josephson junction studied by transmission electron microscopy, *Appl. Phys. Lett.* **75**, 2470.

Wollman, D. A., van Harlingen, D. J., Giapintzakis, J., and Ginsberg, D. M. (1995) Evidence for $d_{x^2-y^2}$ Pairing from the Magnetic Field Modulation of $YBa_2Cu_3O_7$-Pb Josephson Junctions, *Phys. Rev. Lett.* **74**, 797.

Wollman, D. A., van Harlingen, D. J., Lee, W. C., Ginsberg, D. M., and Leggett, A. J. (1993) Experimental determination of the superconducting pairing state in YBCO from the phase coherence of YBCO-Pb dc SQUIDs, *Phys. Rev. Lett.* **71**, 2134.

Zenchuk, A. and Goldobin, E. (2004) Analysis of ground states of 0-π long Josephson junctions, *Phys. Rev. B* **69**, 024515.